Spoke: A 120-kD Protein Associated with a Novel Filamentous Structure on or Near Kinetochore Microtubules in the Mitotic Spindle

Michael R. Paddy* and Daniel Chelsky

Central Research and Development Department, E. I. DuPont de Nemours & Co., Wilmington, Delaware 19880-0328; and *Structural Biology Unit, Howard Hughes Medical Institute and Department of Biochemistry and Biophysics, University of California, San Francisco, California 94143-0554

Abstract. We have characterized an antiserum that recognizes a single 120-kD protein in CHO cells which is soluble and cytoplasmically localized in interphase, but which is associated with a novel filamentous structure localized on or near kinetochore microtubules in mid-mitosis. These filaments, one per sister chromatid, run from near the mitotic spindle pole to within ~0.3 μm of each kinetochore. In metaphase, the staining pattern shows considerable substructure at light microscopy resolution, appearing as bright nodes or striations, often with a kinked or helical appearance. This overall localization pattern is retained throughout anaphase, with the filaments shortening as the chromosomes move toward the mitotic spindle poles. Also in anaphase, a separate ring-like structure lacking a tubulin-staining component appears near the spindle poles. As cells exit mitosis, the amount of this antigen in the cell decreases seven- to tenfold. The unusual staining pattern and the specific localization of this antigen on or near kinetochore microtubules in mid-mitosis indicate that the 120-kD protein defines or is associated with an important and previously unrecognized structural element of the mitotic spindle.

CHROMOSOME segregation during eukaryotic cell division involves the complex spatial and temporal coordination of multiple sets of microtubule structures. These structures are aggregately known as the mitotic spindle apparatus. Of special interest are the kinetochore microtubules, discrete microtubule bundles formed between the poles of the spindle apparatus and the kinetochores of each chromosome (for review see Rieder, 1982). These filaments appear to be essential for chromosome movement from prometaphase through anaphase (for review see Mitchison, 1988). Such movements are postulated to be driven either by the free energy of depolymerization of microtubules at the kinetochore (see, for example, Koshland et al., 1988) or by force generating molecules (the so-called "motors") residing in the kinetochore microtubule bundle or in the kinetochore itself (Nicklas, 1989; Rieder et al., 1990). Despite enormous interest, the molecular components of any such motors remain largely unknown. Currently, models with the motor residing in the kinetochore are popular, particularly with the recent demonstration of dynein being localized to the kinetochore through at least the early stages of mitosis (Pfarr et al., 1990; Steuer et al., 1990). However, alternate models in which fibers adjacent to the kinetochore microtubules provide the force necessary for chromosome movement have long been proposed (see, for example, Forer, 1988). Clearly, the identification and characterization of proteins localized specifically to the kinetochore or kinetochore microtubules could prove essential to an understanding of the mechanisms by which chromosomes move.

In this paper we describe a structurally novel mitotic spindle-associated protein identified in CHO cells while screening antisera for an unrelated project. This protein has a mass of 120 kD (p120), is soluble and cytoplasmically localized during interphase, and becomes primarily associated with the mitotic spindle in mid-mitosis. The use of high resolution, multiple-frequency, three-dimensional digital fluorescence light microscopy (LM;[1] for a recent review, see Agard et al., 1989) has allowed rapid and quantitative descriptions of the localization pattern of this protein alone and relative to known mitotic spindle components. In metaphase, this protein is localized to a series of filaments, one per sister chromatid, which run from near the mitotic spindle pole to near the kinetochore of each chromosome. These filaments appear to be localized on or near kinetochore microtubules at LM resolution, but display substructural features decidedly different from the kinetochore microtubules themselves. Biochemically, the total amount of the p120 antigen in the cell decreases dramatically after anaphase so that little is detectable by the next interphase. Taken together, the data suggest that this protein defines or is associated with an important and previously unrecognized structural component of the mitotic spindle.

Materials and Methods

Antibody Production

The peptide Cys-Gly-Tyr-Gly-Val-Ser-Arg-Lys-Arg-Pro-Arg-Pro-Gly-$CONH_2$,

1. *Abbreviations used in this paper*: DAPI, 4',6-diamidino-2-phenylindole; LM, light microscopy.

designated peptide P2, was synthesized and purified as described previously (Chelsky et al., 1989). The purified peptide was coupled to keyhole limpet hemocyanin (Sigma Chemical Co., St. Louis, MO) using *m*-maleimidobenzoyl-N-hydroxysuccinimide ester (MBS; Pierce Chemical Co., Rockford, IL) (Lanford et al., 1986; Kitagawa and Aikawa, 1976) and injected into three rabbits with complete Freunds adjuvant followed by boosts with incomplete Freunds adjuvant. One rabbit produced the antiserum used in these experiments (Ab-P2), and this antiserum was typically used without further purification. Antibody binding to p120 in immunoblots or to spoke in immunofluorescence cannot be blocked by the free peptide or by the peptide coupled to hemocyanin. It is therefore possible that the P2 peptide is unrelated to the antibody described here. Preimmune serum was not obtained from this rabbit.

Antibody Affinity Purification

Whole cell extracts from 5×10^7 CHO cells were fractionated by SDS gel electrophoresis on a 7.5% acrylamide gel and transferred to nitrocellulose. The region of the nitrocellulose containing p120 as well as a control region containing proteins of ~90 kD were then separately used to adsorb antibody from 20 μl of the Ab-P2 antiserum following the procedure of Earnshaw and Rothfield (1985). The immuno-adsorbed antibody was then eluted, dialyzed, and used without further dilution for immunofluorescence.

Tissue Culture

CHO cells were grown in MEM alpha medium (Gibco Laboratories, Grand Island, NY) plus 10% FCS in 150-cm^2 culture flasks. Mitotic cells were collected by successive shake-offs. Cells were occasionally treated with nocodazole (40 ng/ml) (Sigma Chemical Co.) for 4 h to enhance the proportion of mitotic cells in the population. In this case, collected cells were washed free of nocodazole and placed back in normal medium in the incubator to recover for 0–2 h depending on the experiment. No differences were observed in the fluorescence LM staining patterns of the nocodazole-treated and untreated cells after nocodazole removal and recovery.

Fluorescence LM Sample Preparation

Mitotic cells were spun out of growth medium, resuspended in PBS (10 mM sodium phosphate, pH 7.4, and 0.9% sodium chloride), and applied in 100-μl aliquots to number 1.5 "gold seal" coverslips (Clay Adams, Parsippany, NJ). The coverslips were set into 6-well culture plates on damp filter paper circles and spun in a Sorvall RT-6000 centrifuge (DuPont Co., Wilmington, DE) at 5°C until the rotor reached 1,000 rpm, at which time the run was terminated. Alternatively, cells were placed on coverslips that had been treated with 1 mg/ml polylysine (40 kD, Sigma Chemical Co.) for 10 min. In this case, centrifugation was not necessary and cells were washed after 10 min on ice with PBS. Following either procedure, coverslips were treated with 3.7% formaldehyde in PBS for 10 min, then washed and treated with 0.5% Triton X-100 (Pierce Chemical Co.) for 10 min. This and all subsequent steps were carried out at 25°C. Formaldehyde stock solution (37%) was prepared fresh immediately before use from paraformaldehyde powder (Polysciences, Inc., Warrington, PA) as described previously (Paddy et al., 1990). The Triton and all subsequent solutions were prepared in buffer A, a high potassium, polyamine buffer originally described by Burgoyne et al. (1971) which Sedat, Agard, and co-workers have found optimal for preserving chromatin structure using both EM and LM criteria (Belmont et al., 1989; Sedat and Manuelidis, 1978). As used here, buffer A is 60 mM KCl, 15 mM NaCl, 0.5 mM spermidine, 0.15 mM spermine, 1.5 mM β-mercaptoethanol, 2 mM EDTA, 0.5 mM EGTA, and 15 mM 1,4-Piperazinediethane sulfonic acid adjusted to pH 7.4. Fixed and permeabilized cells were blocked with 10% normal goat serum (Gibco Laboratories) for 20 min followed by a 1:100 dilution of Ab-P2 for 1 h. After rinsing, rhodamine-conjugated affinity-purified goat anti-rabbit IgG $F(ab')_2$ second antibody (Pel-Freeze, Rogers, AR) was applied at 1:200 dilution for 1 h. After rinsing, samples were then stained with either a monoclonal mouse α-tubulin antibody (Amersham Corp., Arlington Heights, IL) at 1:200 or human Crest anticentromere antibody (a generous gift of Karen Butner and Marc Kirschner, Department of Biochemistry and Biophysics, University of California at San Francisco) at 1:800 followed by either fluorescein-labeled affinity-purified goat anti-mouse IgG, $F(ab')_2$ (Pel-Freeze) or goat anti-human IgG, $F(ab')_2$ secondary antibodies (Jackson ImmunoResearch Laboratories, West Grove, PA), respectively. Staining for each antigen was done sequentially since we found that the goat anti-rabbit IgG cross-reacts slightly with the mouse monoclonal α-tubulin antibody. After washing, all samples were stained for 5 min with 4',6-diamidino-2-phenylindole (DAPI), washed again, and rinsed sequentially with 10, 20, 40, 60, and 80% glycerol. Coverslips were then inverted onto 2% *n*-propyl gallate in 90% glycerol (Giloh and Sedat, 1982).

All images shown are from cells fixed with 3.7% formaldehyde. Fixation with either formaldehyde plus 1% glutaraldehyde (Polysciences, Inc., Warrington, PA) or with methanol/acetone (1:3) produced equivalent Ab-P2–stained images. However, glutaraldehyde increased background fluorescence while methanol/acetone resulted in poor preservation of chromosomes.

Three-dimensional LM Data Collection

Three-dimensional LM datasets were collected using a 60×/NA 1.4 oil immersion lens and a modified Olympus IMT-2 inverted light microscope in which the focal position, excitation lamp shutter, excitation and emission barrier filters, and digital camera shutter were under the control of a standalone computer workstation. The dichroic mirrors (Omega Optical, Brattleboro, Vermont) were tuned to pass two sets of excitation and emission wavelengths. The index of refraction of the immersion oil (n_D = 1.5150) was chosen to minimize spherical aberration in the image (Hiraoka et al., 1990). LM images were digitized directly from the microscope image plane using a 12 bit, Peltier-cooled charge coupled device (CCD) digital camera (Photometrics, Tucson, Arizona). This instrument has been described briefly previously (Hiraoka et al., 1989) and was built in the laboratories of Drs. John W. Sedat and David A. Agard with the generous support of the Structural Biology Unit of the Howard Hughes Medical Institute.

For all samples, pairs of complete three-dimensional datasets at two fluorescence wavelengths were recorded simultaneously. That is, two optical sections at different fluorescence wavelengths were collected at the same focal position using the computer-controlled barrier filters and the doubly tuned dichroic mirrors before moving the focal position to record another pair of optical sections. Three-dimensional datasets were collected as 512 × 512 pixel images (0.074 × 0.074 μm pixel size, yielding a total image size of 38 × 38 μm) separated by 0.1 μm along the optical sectioning axis. Each three-dimensional dataset contained 50–100 optical sections.

Datastack Preprocessing and Computational Removal of Out-of-Focus Information

After data collection and before beginning the three-dimensional deconvolution to remove the out-of-focus information, each three-dimensional LM dataset was corrected for fluorescence photobleaching through the dataset, lamp intensity and/or shutter open time variations, and stage and/or sample drift, as described previously (Paddy et al., 1990), after including a correction for small but systematic failures of the correction file to flat-field the image (Swedlow, J. R. S., J. W. S. Sedat, and D. A. A. Agard, unpublished results). The great majority of the out-of-focus contamination was removed using a Fourier-based iterative, constrained three-dimension deconvolution method (Agard et al., 1989) incorporating the experimentally measured point spread function for the microscope (Hiraoka et al., 1990). Deconvolutions were allowed to run for 25 iterations.

Image Display and Three-dimensional Modeling

Three-dimensional LM images were displayed and modeled using an integrated, multiple-windowed, mouse-driven display and modeling program specially designed for analyzing complex, three-dimensional biological structures (PRISM; Chen et al., 1989). Displays of multiply-labeled samples used a version of PRISM employing a 24-bit display (8 bits or 256 grey levels for each of the red, green, and blue primary display colors).

Centromere to centromere distances in the three-dimensional models were made using a distance calculation routine inside the modeling program. Centromere to spoke protein filament tip distances in these models were made from listings of coordinates after assigning centromere–filament tip pairs inside the modeling program.

Registration of Multiple Images from the Same Sample

In multiply-labeled samples for the LM, the Sedat and Agard laboratories have found it necessary to correct for the three-dimensional translations caused by changing the barrier filter optical elements and to correct for wavelength-dependent magnification changes (see, for example, Paddy et al., 1990). For the tissue culture cell samples used in this study, these correction factors appear to be adequately determined from separate samples of small fluorescence beads in glycerol (for a cautionary counter-example in *Drosophila* embryos, see Paddy et al., 1990).

The translation and magnification correction factors were determined from a 1/10 water dilution of 0.07 ± 0.009 μm Fluoresbrite™ latex beads (Polysciences, Inc.) allowed to dry on a number 1.5 coverslip before inverting onto 2 μl of 2% *n*-propyl gallate/90% glycerol/10% buffer A on a glass microscope slide. Pairs of three-dimensional fluorescence LM datasets were collected as above for fluorescein/sulforhodamine and DAPI/rhodamine pairs in triplicate (i.e., 12 datasets total), with removal and reinsertion of the double dichroic mirror from the microscope between each data collection set. The translation and magnification correction parameters were determined using a Fourier-based, phase-dominated cross correlation scheme which determined the translation factors maximizing the cross correlation intensity as a function of magnification correction in the x,y (focal) plane (Shaw et al., 1989; Swedlow, J. R. S., J. W. S. Sedat, and D. A. A. Agard, unpublished results). That magnification correction factor producing the global maximum in the cross correlation function and the corresponding translation factors were used as the translation and magnification correction factors. In triply labeled samples, the very similar rhodamine and sulforhodamine datasets from the different dichroic dataset pairs were used to align the two pairs of three-dimensional datasets via the cross correlation alignment scheme described above.

p120 Antigen Quantitation through the Cell Cycle

CHO cells were blocked in early prometaphase by treatment with nocodazole. Mitotic cells were shaken off, washed free of nocodazole, aliquoted, and returned to the incubator. A gyrating platform (Nutator; Clay Adams) was used to maintain the cells in suspension. At the indicated times, cells were centrifuged out of their medium, solubilized in buffer B (20 mM sodium phosphate, pH 7, 0.2% aprotinin, 5 μg/ml protease inhibitor cocktail (chymostatin, leupeptin, antipain, and pepstatin), 1 mM PMSF, and 0.5% Triton X-100) with 20 μg/ml taxol (a gift of Dr. Karl Flora, National Institutes of Health, Bethesda, MD) and microfuged for 2 min at full speed. The resulting supernatant and pellet fractions were then assayed by SDS gel electrophoresis, transfer to Immobilon P (Millipore Continental Water Systems, Bedford, MA), and immunoblotting with spoke antiserum at a dilution of 1:1,000. Bands were visualized with ^{125}I-protein A (DuPont Co.) and autoradiography. Densitometry was used for quantitation of the resulting bands.

Aliquots of cells from each time point were also dropped onto coverslips coated with polylysine and fixed after 5 min on ice with 3.7% formaldehyde for 10 min at 25°C. Fixed cells were then rinsed and permeabilized with 0.5% Triton X-100 for 10 min, rinsed and stained with DAPI for 5 min, and rinsed and examined by fluorescence microscopy. All solutions were made in PBS.

Gel Filtration

Interphase or mitotic CHO cells (2×10^7) were lysed in 10 mM Tris, pH 7.5, 50 mM NaCl, and 5 μg/ml of protease inhibitor cocktail. After centrifugation at 30,000 *g* for 5 min, the supernatant was loaded onto an AcA 34 gel filtration column (LKB Instruments Inc., Bromma, Sweden). Protein standards were added to the sample for determination of apparent mass (thyroglobulin, 669 kD; apoferritin, 443 kD; β-amylase, 200 kD; alcohol dehydrogenase, 150 kD; BSA, 67 kD). Fractions from the column were assayed for p120 by gel electrophoresis and immunoblotting as described above.

Results

A Novel Mitotic Spindle Component Observed in Metaphase

During the routine screening of several antinuclear transport peptide antisera (see Materials and Methods), one antiserum (Ab-P2) was found to recognize a single protein of ~120 kD (p120) in CHO cells after SDS gel electrophoresis and immunoblotting (Fig. 1 *A*). When interphase CHO cells are lysed by homogenization under conditions that do not disrupt the nuclei as judged by phase-contrast microscopy, p120 appears entirely in the supernatant fraction after high speed centrifugation (Fig. 1 *A*, lanes *3* and *4*). When mitotic cells are treated in the same way, p120 is distributed in both the

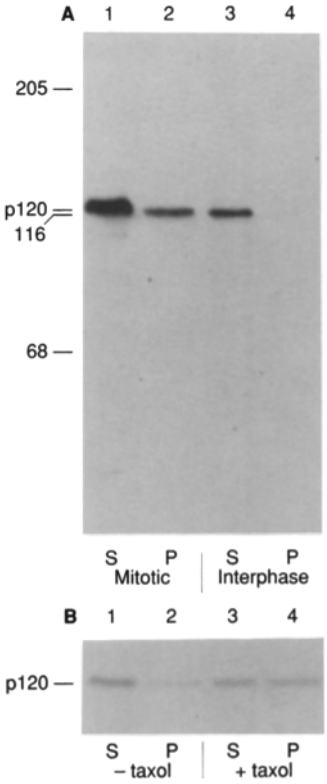

Figure 1. Ab-P2 antiserum recognizes a single 120-kD protein in CHO cells with a cell cycle–dependent cellular localization. CHO cells were treated with the microtubule inhibitor nocodazole to increase the fraction of mitotic cells. Mitotic cells were shaken off after 4 h and the interphase cells that remained were scraped off. Equal numbers of mitotic and interphase cells (10^6) were then washed in PBS, homogenized in 0.1 ml of buffer B, and centrifuged at 10,000 *g* for 2 min. The supernatant and pellet fractions were solubilized and analyzed by SDS-gel electrophoresis and immunoblotting with the Ab-P2 antiserum. (*A*) Distribution of p120 in interphase and metaphase. (lane *1*) Mitotic cell supernatant; (lane *2*) mitotic cell pellet; (lane *3*) interphase supernatant; (lane *4*) interphase pellet. (*B*) Effect of the microtubule stabilizing agent taxol in the lysis buffer on the distribution of p120 in metaphase. (lane *1*) Nontaxol supernatant; (lane *2*) nontaxol pellet; (lane *3*) taxol supernatant; (lane *4*) taxol pellet. (*S*) Supernatant fraction; (*P*) pellet fraction. Protein standards were BSA (68 kD), β-galactosidase (116 kD) and myosin (205 kD).

supernatant and pellet fractions (Fig. 1 *A*, lanes *1* and *2*). The same results are obtained whether or not cells are treated with the nonionic detergent NP-40 before centrifugation, indicating that association with the pellet fraction in mitotic cells is not likely to be membrane related. Treatment of mitotic cells with the microtubule stabilizing agent taxol during lysis (Kuriyama et al., 1984) results in an increase of p120 associating with the pellet fraction from 18 to 43% (Fig. 1 *B*).

Three-dimensional fluorescence LM using the anti-p120 serum reveals an unusual structure in mitotic CHO cells that appears filamentous and spoke-like, as shown for six individual cells in Fig. 2. This staining pattern has led us to designate the p120 protein as "spoke". The cells shown in Fig. 2 were collected by mechanical shake-off from tissue culture flasks and centrifuged onto glass coverslips. Most cells in this panel were treated with the microtubule inhibitor nocodazole before shake-off to increase the quantity of mitotic cells (Zieve et al., 1980). In the presence of nocodazole, neither spoke nor tubulin filaments are observed. After nocodazole removal and recovery, however, no differences are observed between these cells and those never treated with nocodazole. The images in Fig. 2, *a–h* are projections of multiple adjacent fluorescence LM optical sections (see figure legend) which have been processed to significantly reduced the out-of-focus information that obscures the image in each focal plane (Agard et al., 1989). The top row of Fig. 2 shows the anti-spoke and corresponding DAPI-stained

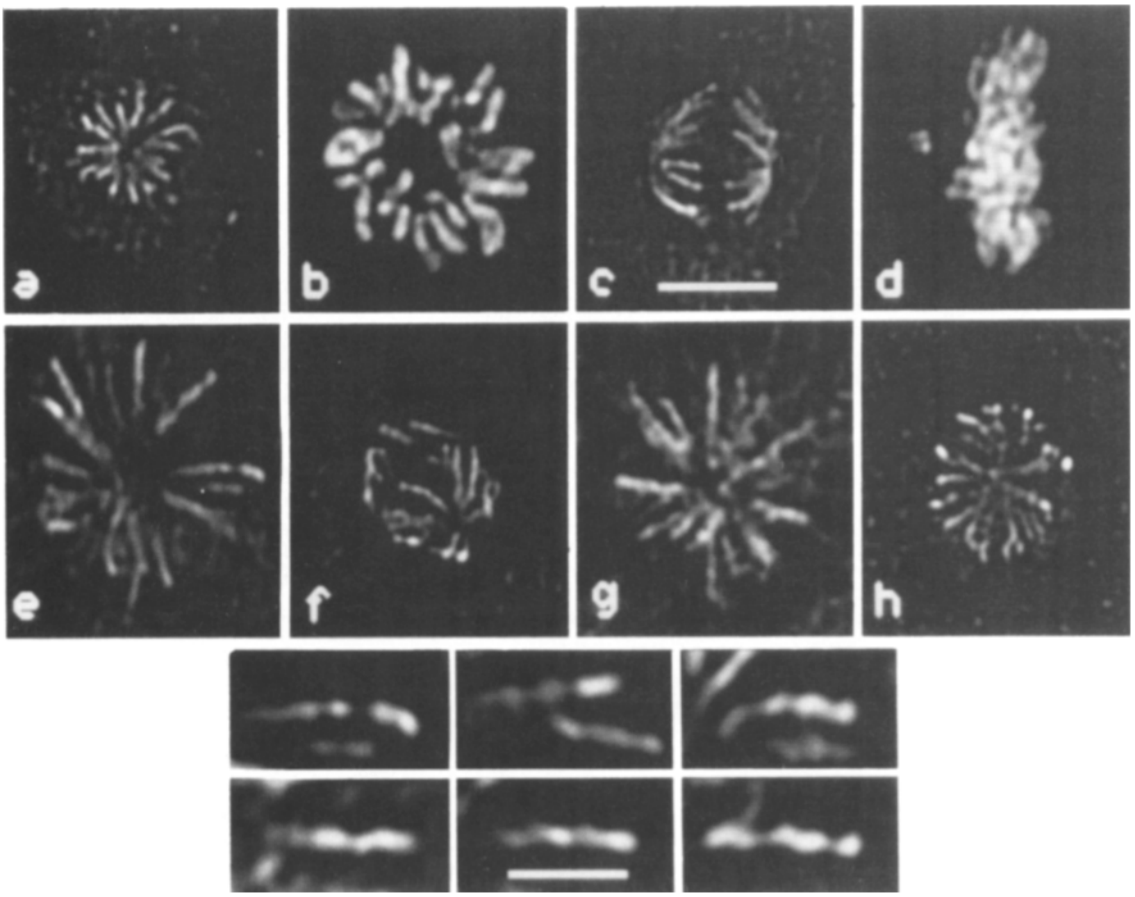

Figure 2. A novel structure is observed by fluorescence LM in the mitotic spindle of Ab-P2-stained CHO cells. (*a*) Ab-P2-stained metaphase cell with the mitotic spindle axis perpendicular to the image plane; (*b*) the same cell as in *a* stained with DAPI; (*c*) Ab-P2-stained metaphase cell with the spindle axis parallel to the image plane; (*d*) the same cell as in *c* stained with DAPI; (*e–h*) four metaphase cells stained with Ab-P2; (*six lower panels*) details from the images in *e–h*. Each image is a projection of from 5 to 27 contiguous 0.1-μm optical sections. The local contrast in these images has been enhanced as described previously (Belmont et al., 1987). Bars: (*a–h*) 4.0 μm; (*six lower panels*) 2.0 μm.

chromosome images for two mitotic CHO cells in which the mitotic spindle axis is oriented perpendicular (Fig. 2, *a* and *b*) or parallel (Fig. 2, *c* and *d*) to the image plane. The antispoke staining pattern shows two symmetric sets of filaments radiating from near the mitotic spindle poles to the chromosomes, forming two basket-like structures. These fiber-like structures do not join at the spindle poles nor meet at the metaphase plate.

Counting the number of antispoke-stained fibers in these metaphase cells suggests that there is one fiber per sister chromatid. To quantitate the number of fibers, a three-dimensional modeling program designed for complex biological structures was used, which allowed simultaneous viewing of multiple orientations of the three-dimensional data set (Chen et al., 1989). From the models of the antispoke staining in three mitotic cells (a representative model is shown in Fig. 4, *d* and *e*), we counted 36, 40, and 40 fibers per cell. Given that the diploid (2n) number of chromosomes in these cells is typically 20 with a range of 18–22 (Hay et al., 1983), the fiber numbers obtained correspond to one per sister chromatid in these mitotic (4n) cells. We directly confirmed this relationship using anticentromeric antibodies (see next section).

As shown in the LM projection images in Fig. 2, *e–h*, the antispoke staining pattern does not appear smooth and uniform along each fiber, but instead has considerable substructure. Details of these substructural patterns are shown in the six enlarged images at the bottom of Fig. 2. Staining along the fiber path most often appears as a series of regularly spaced, brightly stained regions with weaker staining in between. The staining often, but not always, appears to have a kinked or coiled component. Irrespective of the precise nature of the staining pattern, however, it is clear that these features represent a distinctly different staining pattern from the relatively simple, continuous, and linear pattern obtained from antitubulin staining in microtubules (see next section).

The distance between the kinks in the fiber path or the bright regions or nodes of staining on the fibers appears fairly uniform within any one cell. This distance, however, varies from cell to cell but may be uniform when normalized by filament length. For example, a cell with spoke-associated filaments of 1.55 ± 0.08 μm in length (seven filaments measured) was found to have internodal distances of 0.39 ± 0.04 μm (eight internodal distances measured), while a second cell with filaments of 2.13 ± 0.11 μm in length (seven filaments measured) was found to have internodal distances of

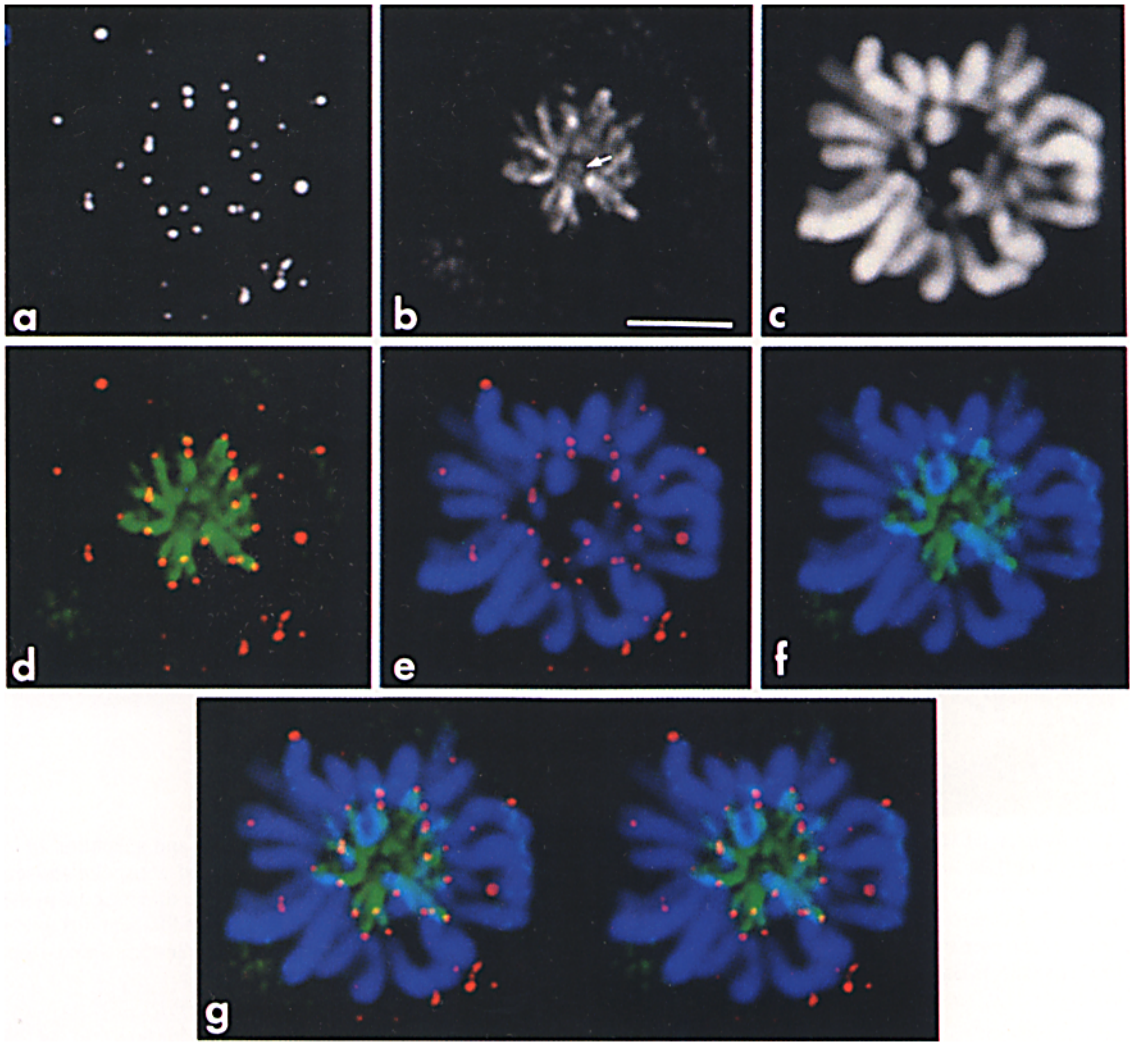

Figure 3. Spoke-associated filaments extend from a region near the spindle poles to near the centromere of each chromosome. Fluorescence LM images from approximately one-half spindle of an early anaphase CHO cell stained for chromosomes, centromeres, and spoke. (*a–c*) Single component staining patterns: (*a*) anticentromere; (*b*) antispoke; and (*c*) DAPI-stained chromosomes. (*d–f*) Pairwise superpositions of the individual staining patterns: (*d*) centromeres and spoke; (*e*) centromeres and chromosomes; (*f*) spoke and chromosomes. (*g*) ±5° stereo pair of the superposition of all three staining patterns. Color scheme for all the superposition images: (*red*) centromeres; (*green*) spoke; and (*blue*) chromosomes. Other hues result from the overlap of these three colors. Each image is a projection of 20 contiguous 0.1-μm optical sections. Bar, 4 μm.

0.54 ± 0.03 μm (11 internodal distances measured). The ratio of internodal distance to filament length in these two cells has the same value of 0.25. The range in internodal distance in different metaphase and early anaphase cells is roughly estimated as 0.4–0.7 μm (note the large variation in the overall spoke-associated filament lengths in Fig. 2). The total number of these bright features on a given filament is difficult to estimate in all cells since many of the fibers appear to overlap each other. In many cells, however, there appear to be about five per filament, as can be seen in the lower panels of Fig. 2.

To correlate immunoblotting results with the fluorescence LM staining pattern, antibodies specific for only p120 were purified from the total antiserum. Whole CHO cell extracts were fractionated by gel electrophoresis and transferred to nitrocellulose. The 120-kD region as well as a control region containing proteins of ~90 kD were then separately used to adsorb antibody from the Ab-P2 antiserum following the procedure of Earnshaw and Rothfield (1985). Immunofluorescence staining patterns from this affinity-purified antiserum give indistinguishable results from the complete Ab-P2 serum. Antibody purified from the 90-kD region of the nitrocellulose produces no detectable signal.

Localization of Spoke Relative to Known Mitotic Spindle Components in Metaphase and Early Anaphase

To determine the spatial relationships between the spoke staining pattern and other known components of the mitotic spindle, we have multiply stained metaphase CHO cells for the fluorescence LM with antispoke, DAPI, an anti-α-tubulin mAb, and a human scleroderma CREST serum that recognizes centromeres. Due to the limited number of fluorophores available to us, we have stained only three compo-

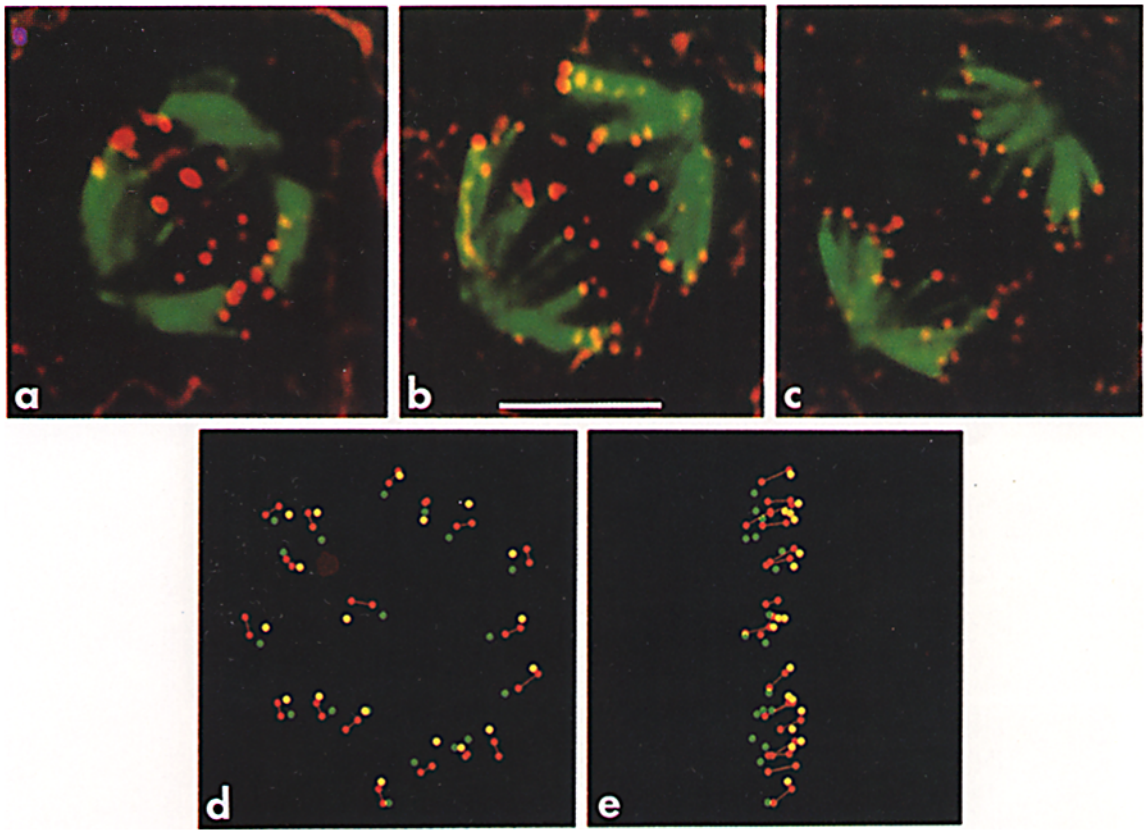

Figure 4. Centromeres remain in close proximity to the tips of the spoke-associated filaments throughout metaphase and anaphase. (*a–c*) Superpositions of fluorescence LM image projections of three anaphase cells stained with anticentromere (*red*) and antispoke antisera (*green*). Each image is a projection of 24, 26, or 28 contiguous 0.1-μm optical sections. (*d* and *e*) Projections of a three-dimensional model built from the fluorescence LM datasets of a metaphase cell (images not shown) showing the proximity of spoke protein filament tips (*green or yellow circles*) to the centromeres of each sister chromatid (*red circle pairs*). Two projections are shown: along the mitotic spindle axis (*d*) and orthogonal to this axis (*e*). Bar, 4 μm.

nents in a cell at any one time. That is, cells were stained with antispoke, DAPI, and either the anti-α-tubulin antibody or the centromere-recognizing serum. Before beginning analysis, the three datasets were aligned by correcting for wavelength-dependent translation differences and magnification changes (see Materials and Methods).

Fig. 3 shows an early anaphase CHO cell viewed down the mitotic spindle axis after staining for spoke, chromosomes, and centromeres. The three LM projection images in the top row (Fig. 3, *a–c*) show the staining patterns for each of these components alone in approximately one-half spindle. The remaining images in Fig. 3 are superpositions of these three images. Fig. 3 *a* shows that this centromere-staining antiserum also stains a number of epitopes in the cell periphery. However, by comparing this staining pattern to the centromeric constriction points of the chromosomes (Fig. 3 *e*), one readily observes that this serum acts as a reliable marker for centromeres in the vicinity of the chromosomes. Superposition of spoke and centromere staining patterns (Fig. 3 *d*) clearly shows that the spoke signal terminates at or very near the centromeric regions. Spatial integration of all three staining patterns demonstrates that spoke-associated fibers travel from a roughly common origin well off the mitotic plate to a position in close contact with the chromosomes at their centromeres (Fig. 3 *g*). Also evident in this figure is a ring-like structure near the spindle pole in the spoke image (*arrow* in Fig. 3 *b*). This feature is seen in all anaphase cells (see also *arrows* in Fig. 5 *f*), is not observed in metaphase (see Fig. 2), and does not appear to be directly connected to the spoke staining in the vicinity of the kinetochore microtubules.

As the chromosomes migrate from the metaphase plate toward the mitotic spindle poles, the spoke staining pattern shortens towards the poles while maintaining close proximity to the centromeres. This relationship in shown in Fig. 4, *a–c*. Displayed here are progressively later stages of anaphase in different CHO cells. Each panel shows a color superposition of projections of all the processed sections from each of the spoke (*green*) and centromere (*red*) images. In all of these images, the dots of centromere staining appear at the chromosomal end of the spoke associated fibers, clearly demonstrating that the ends of these fibers remain near their respective centromeres as the fibers shorten. No significant spoke staining is observed between the centromeres of the sister chromatids in anaphase.

We have quantitated the distance between the centromeres and the tips of the spoke structure by modeling their positions in three-dimensional space using the modeling program described above. Three-dimensional models of filament tip and centromere positions were made separately from data sets

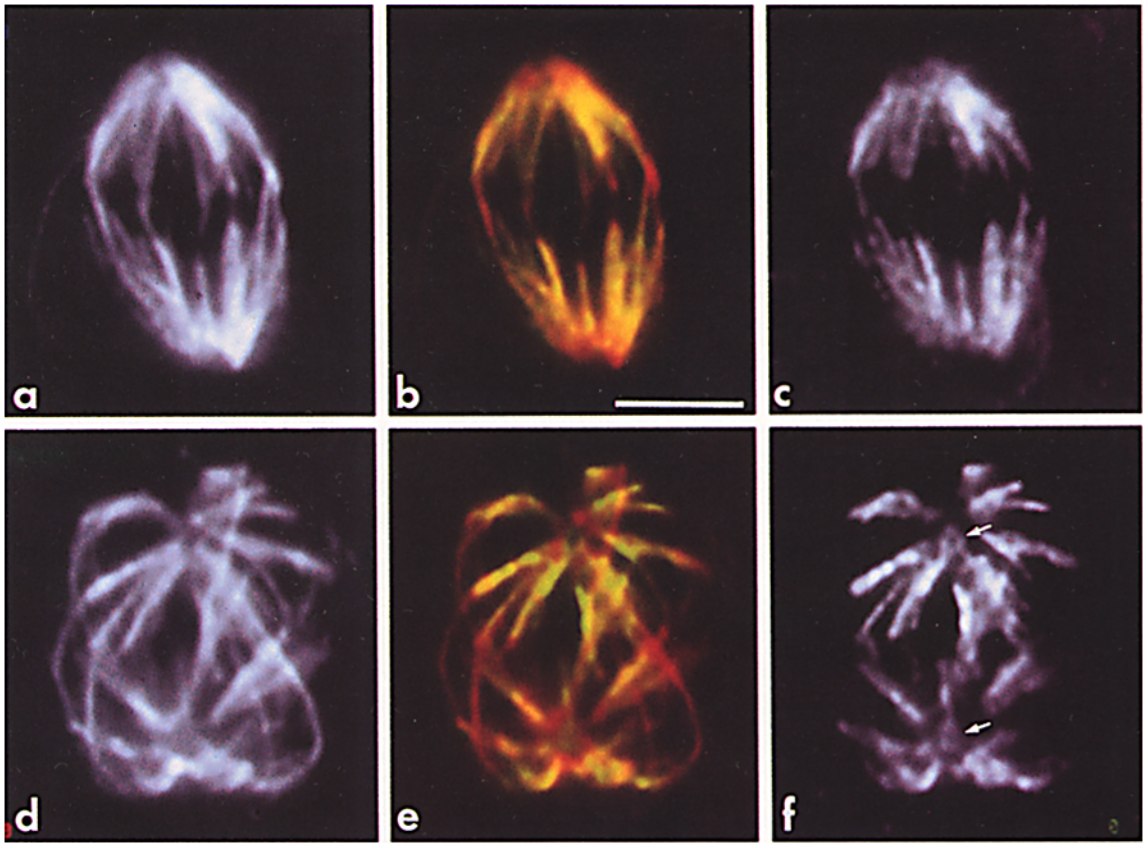

Figure 5. Spoke is localized on or near kinetochore microtubules. Fluorescence LM image projections from two anaphase cells stained with an anti-α-tubulin mAb (*a* and *d*) and the antispoke antiserum (*c* and *f*). (*b* and *e*) Superposition of tubulin (*red*) and spoke (*green*). Yellow regions in the superposition images result from equal intensity contributions from the two components. Each image is a projection of 15 or 28 contiguous 0.1-μm optical sections. Bar, 4 μm.

collected from the same metaphase cell. A superposition of the two independently made models is shown in Fig. 4 in two orientations: parallel to the mitotic spindle axis (Fig. 4 *d*) and perpendicular to the spindle axis (Fig. 4 *e*). The tips of the filaments have been designated as green or yellow solid circles, representing the different half-spindles from which they derived, while the centromeres have been designated as solid red circles.

In nearly all cases, centromere staining is seen as pairs of bright nodes, one on each sister chromatid, with continuous but weaker staining between the nodes. Each chromatid pair is therefore shown as a pair of dots with the connecting line. From this model, the distance between pairs of centromeres is found to be 0.66 ± 0.08 μm, consistent with electron micrograph measurements (Pepper and Brinkley, 1977). The continuous staining observed between each chromatid pair suggests that this anticentromere antibody may be recognizing a CENP-B-like antigen (Cooke et al., 1990).

In the spindle axis view (Fig. 4 *d*), the centromeres approximate a circle 6.5 μm across. One chromosome is out of place in this cell, and is located in the center of the plate, but retains its connection to the spoke-associated fibers. In the orthogonal view (Fig. 4 *e*), one observes very little deviation of the centromeres from the center of the metaphase plate. Near each centromere is a single filament tip. Measuring the distance between the filament tips and the centromeres in the 22 most structurally similar cases (61% of such distances existing in the sample), one obtains a separation distance of 0.31 ± 0.09 μm. The possibility that DNA is interfering with antibody binding in the vicinity of the chromosomes, thereby producing the observed gap between the filament tips and the centromeres, was investigated by treating fixed cells with DNase I before immunostaining. This treatment resulted in elimination of the DNA but the gap between spoke and centromere staining remained (data not shown). The observed separation between the end of the spoke associated filament and the centromere may be expected if the anticentromere antibody recognizes a CENP-B-like antigen (Cooke et al., 1990).

Since antispoke appears to stain a structure which has many of the attributes of kinetochore microtubules, a direct comparison was made between the antispoke staining pattern and that of α-tubulin, a major component of kinetochore microtubules (Fig. 5). A projection of all the processed sections through two anaphase cells are shown, one viewed perpendicular to the mitotic spindle axis (Fig. 5, *a–c*) and one roughly parallel to this axis (Fig. 5, *d–f*). For both cells, the anti-α-tubulin staining pattern is shown at left (Fig. 5, *a–d*), the antispoke staining pattern at right (Fig. 5, *c* and *f*) and a color superposition of the two images in the center (Fig. 5, *b* and *e*). In the superposition image, α-tubulin is shown in red, spoke in green, and equal intensity overlap regions appear as yellow. The majority of the anti-α-tubulin staining pattern in both cells extends from the mitotic spindle poles

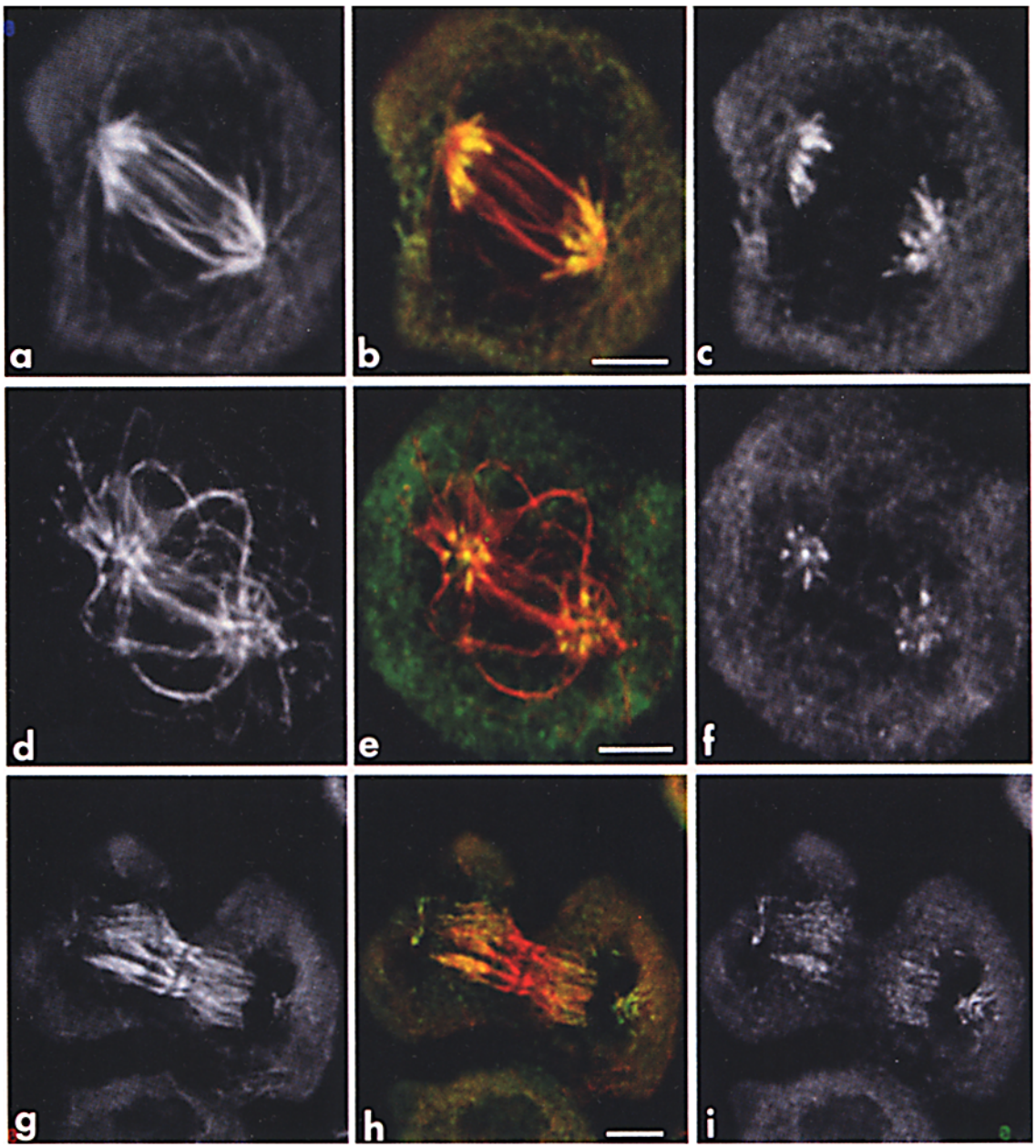

Figure 6. Localization of spoke and tubulin in late anaphase, telophase, and cytokinesis. Three cells stained with anti-α-tubulin antibody and antispoke antiserum. (*a*, *d*, and *g*) Projections of antitubulin images; (*c*, *f*, and *i*) antispoke projections; (*b*, *e*, and *h*) superposition of tubulin and spoke images. Superposition color code is as in Fig. 5. Each image is a projection of 9, 23, or 24 contiguous 0.1-μm optical sections. Bars, 4.0 μm.

to the kinetochore region of the chromosomes, and represents the kinetochore microtubules (Rieder, 1982). Visual comparison of the antispoke and anti-α-tubulin stained images indicates that the two staining patterns are very similar in their localization in the kinetochore microtubule region. Direct superposition of these two images shows extensive regions of overlap (note regions of yellow in Fig. 5, *b* and *e*), indicating that spoke and kinetochore microtubules are proximal or possibly coinciding. Note that the much more extensive substructure in the spoke staining relative to α-tubulin produces an alternating pattern of red and yellow in regions of overlap.

While spoke and tubulin overlap extensively in the kinetochore microtubule region, spoke staining is noticeably absent from the polar microtubules which extend from pole to pole. These microtubules can be seen most clearly where the kinetochore microtubules are not present, such as in the midbody region and near the poles (in particular, see Fig. 5 *e*). In these regions, the polar microtubules appear as red, indicating the absence of spoke.

Visible at the spindle poles and unique to the spoke pattern are the rings of staining. This feature, visible at both poles in Fig. 5 *f* (see *arrows*), appears only in anaphase cells, being noticeably absent in metaphase (see metaphase staining patterns in Fig. 2). Since no tubulin staining is associated with this structure (see Fig. 5 *e*), it appears to represent a new

structure which does not colocalize with known microtubule structures in the spindle.

Spoke Localization Late in Mitosis

Throughout anaphase, the antispoke staining pattern continues to be adjacent to or coincident with kinetochore microtubules. Fig. 6 shows LM projection images for tubulin alone (*left column*), spoke alone (*right column*), and a color superposition of the two images (*central column*). The extensive regions of yellow in Fig. 6 *b* indicate a close localization of spoke and kinetochore microtubules, similar to that observed in Fig. 5 *e*. Note that the polar and astral microtubules in Fig. 6 *a* are not recognized by the spoke antibody (Fig. 6 *c*). Additionally, there is considerable nonuniform spoke staining appearing in the cytoplasm. This staining is maintained into the next interphase (Fig. 6, *f* and *i*). In late anaphase, the spoke staining pattern is reduced to a central spot surrounded by a set of very short filaments (Fig. 6 *f*). Tubulin staining overlaps with this pattern, though the polar microtubules are free of spoke staining (the splayed nature of the polar microtubules in this cell is the result of damage sustained during centrifugation; the unusual orientation, however, gives a clear view of both poles from the top of the cell rather than the typical side-on image). As cells proceed on to cytokinesis, spoke staining remains on the distal edges of the nascent nuclei (Fig. 6 *i*). Note that there is little tubulin staining associated with these polar structures (Fig. 6 *g*). In addition, two new patches of staining appear between the two daughter nuclei that were not visible earlier. These patches appear filamentous and seem to coincide with the more polar portions of the midbody microtubules (see Fig. 6 *h*). Finally, in early interphase, the spoke staining pattern is entirely cytoplasmic, with the nuclear region being essentially devoid of spoke staining (see the half-cell at the bottom of Fig. 6, *g–i*).

p120 Antigen Concentration and Localization Are Cell Cycle Regulated

As mentioned earlier (see Fig. 1 and discussion thereof), spoke is soluble in interphase but becomes significantly although not exclusively associated with the pellet fraction of metaphase cells. Our LM results strongly suggest that the insoluble portion of this protein is associated with kinetochore microtubules. To corroborate this structural result, we have studied the biochemical localization of p120 as a function of time through the mitotic cycle.

The time course of p120 localization in the pellet fraction correlates with mitotic spindle formation and disappearance through mitosis, as shown in Fig. 7. Maximal p120 association with the pellet fraction occurs between 10 and 35 min after release from the nocodazole block (Fig. 7 *A*). The initial increase of p120 in the pellet corresponds to the transition of cells from prophase to metaphase as determined by DAPI staining of the chromosomes (see Fig. 7 *B*). Between 35 and 45 min, the amount of p120 in the pellet falls off rapidly, and corresponds to the transition of most cells from telophase to cytokinesis. The p120 in the pellet fraction then continues to decrease more slowly until it reaches zero at 80 min. The continued presence of p120 in the pellet in telophase and cytokinesis presumably results from the LM-observed association of spoke with the midbody microtubules following the disappearance of the kinetochore microtubules (see Fig. 6 *i*).

It was also observed in the spoke time course (Fig. 7 *A*) that the total amount of the p120 signal in the combined pellet and supernatant fractions changed substantially during the experiment. An initial twofold increase was seen in the first 30 min while a decrease to ~10% of the maximal levels was observed at late times. To determine whether this resulted from processes such as protein degradation, sample

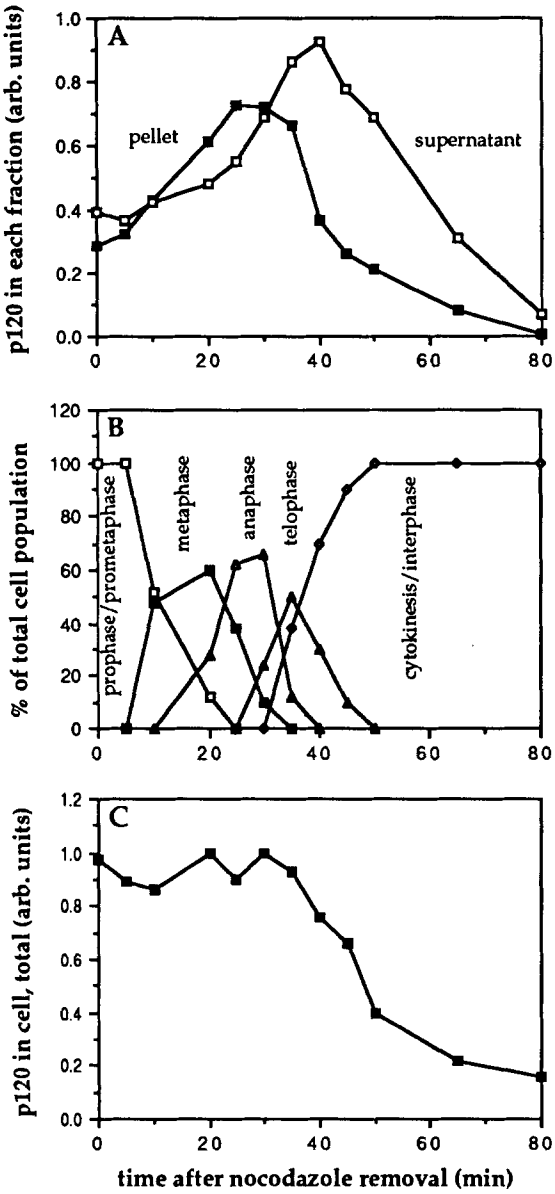

Figure 7. Reduction of total cellular anti-p120 signal after the disappearance of spoke-associated filaments. (*A*) CHO cells were blocked in early prometaphase with nocodazole followed by collection of the mitotic cells and removal of the nocodazole. At the indicated times, equal aliquots of cells were analyzed for p120 distribution in the cell (see Materials and Methods). (*B*) At each time point an aliquot of cells was also taken for fixation, permeabilization, and DAPI staining to determine the fraction of cells in each mitotic cell cycle stage. (*C*) In a similar experiment, aliquots of cells were solubilized directly in SDS before analysis for total p120.

loss, or epitope modification during cell lysis and fractionation, the experiment was repeated without the cell fractionation step. In this case, aliquots of cells were solubilized directly in SDS at each time point before analysis by gel electrophoresis and immunoblotting. While the level of p120 signal remained stable from prometaphase through mid-telophase under these conditions, the p120 signal began to disappear rapidly as cells entered interphase (Fig. 7 *C*). Less than 15% of the original p120 signal remained 80 min after removal of nocodazole. The continued presence of soluble p120 into the next interphase is consistent with the diffuse spoke immunofluorescence in the cytoplasm of interphase cells (see the half cell at the bottom of Fig. 6 *i*). In the case of the Western blotting as well as the immunofluorescence, it should be noted that we cannot readily distinguish between epitope modification and degradation of the protein. In either case, it is apparent that a change is taking place during the transition from mitosis to G_1.

To determine the aggregation state or possible associations of the soluble form of the spoke protein, we fractionated protein from interphase cells on a gel filtration column. Under these conditions, the antispoke reactive band migrated primarily with an apparent mass of 480 kD along with a lesser amount of protein migrating with an apparent mass of 240 kD (data not shown), as compared with spoke under denaturing conditions at 120 kD (see Fig. 1). The same results were obtained with the soluble fraction from mitotic cells.

Discussion

In this paper we describe a novel 120-kD protein which is localized on or near kinetochore microtubules in metaphase. When viewed through the mitotic spindle poles using immunofluorescence LM, the staining pattern has a spoke-like appearance for which we have named this protein. During anaphase, spoke-associated filaments retain the same overall structural pattern, but become progressively shorter as the chromosomes migrate toward the mitotic spindle poles, until the fibers completely disappear in telophase. Biochemically, we observe an entirely consistent result in that after cell lysis the p120 protein partitions with the pellet fraction, which contains the spindle. Taxol, which stabilizes microtubules, also significantly increases p120 partitioning with the pellet. As cells move out of mitosis, the amount of p120 in the pellet drops to zero, again consistent with the LM observations.

A distinctive feature of the spoke immunofluorescence LM staining pattern is the variable staining intensity along each spoke-associated filament. Tubulin staining is generally seen as uniform with occasional and irregular variations in staining intensity (see Figs. 5 and 6). Spoke staining, on the other hand, is decidedly nonuniform and is typically seen as roughly regularly spaced, brightly staining regions connected by areas of reduced intensity (see especially Figs. 2 and 5). The net effect is a striated, kinked or helical appearance. This appearance may represent a discontinuous localization pattern, such as that observed in muscle fibers, or possibly a coiled structure wrapping around the kinetochore microtubules. Further interpretation should await observations at EM resolution.

An interesting but less well documented aspect of the spoke staining pattern is the periodicity of the striations, kinks, or coils. In the limited number of cells that have been quantitated, the number of bright regions along each filament is fairly uniform even though filament length varies from cell to cell. When comparing cells with differing filament lengths, the periodicity of the bright features is proportional to filament length. This very preliminary finding is consistent with a dynamic structure capable of determining or reacting to the dimensions of the filamentous bundle with which it appears associated.

Another distinctive feature of the spoke staining pattern is a ring or hub-like structure near the convergence of the spoke associated filaments at the mitotic spindle poles (see *arrows* in Figs. 3 and 4). This structure is not stained by anti-α-tubulin antibody and therefore does not appear to be a component of the kinetochore microtubules. The spoke-associated filaments generally do not connect directly to this ring. The ring structure is observed only during anaphase and it has not been observed in metaphase or telophase cells. This region may be the pericentriolar area which is a site of microtubule initiation.

In late anaphase and telophase, spoke staining can be seen in the vicinity of the polar region of the midbody microtubules (see Fig. 6 *h*). This staining is reduced in intensity from that observed on the kinetochore microtubules. It does not appear to represent remnants of spoke-associated filaments lost during depolymerization at the kinetochores, since we only observe this pattern very late in anaphase and the staining does not appear in the region formerly occupied by the kinetochore microtubules. It may be that spoke is associating with the polar region of these midbody microtubules after depolymerization of the kinetochore microtubules. Other mitotic spindle antigens are also known to redistribute to the midbody microtubules in telophase. These include calmodulin (Welsh et al., 1979), myosin light chain kinase (Guerriero et al., 1981) and the inner centromere protein (INCENP; Cooke et al., 1987). In the midbody microtubules, calmodulin appears to have roughly the same localization pattern as spoke, while the two other proteins localize to the central region rather than the polar ends.

The macromolecules responsible for chromosome movement have not been identified. However, at least two proteins with this potential have been found in the mitotic spindle. Cytoplasmic dynein, which transports organelles to the minus end of microtubules, has been shown to localize to the kinetochores and spindle fibers of mammalian cells during mitosis (Pfarr et al., 1990; Steuer et al., 1990). As with spoke, dynein is found in the cytoplasm during interphase. Kinesin, which is capable of transporting organelles to the plus end of microtubules, has been detected in sea urchin mitotic spindles (Scholey et al., 1985) as well as the spindle poles of mammalian cells (Neighbors et al., 1988). While spoke in CHO cells has the same apparent molecular weight under denaturing conditions as the large chain of cytoplasmic kinesin, it does not appear to be cytoplasmic kinesin by two criteria. First, the two proteins differ in size under nondenaturing conditions. In gel filtration analysis, the soluble form of spoke migrates with an apparent mass of 480 kD along with a minor component at 240 kD (apparent tetramers and dimers, respectively), while native kinesin is reported to migrate under similar conditions with an apparent mass of 800 kD (Bloom et al., 1988). Secondly, the localization patterns of spoke and cytoplasmic kinesin in mammalian cells appear to differ (Neighbors et al., 1988). This does not mean that spoke may not show homology to kinesin in some important functional domain. Recently, two nuclear proteins

have been reported in fungi (Enos and Morris, 1990; Meluh and Rose, 1990) which show homology with kinesin in only the "motor" portion of the proteins. Also, at the *claret* locus in *Drosophila*, a kinesin-like protein has been identified that is necessary for normal chromosomal segregation in meiosis and early mitotic divisions of the embryo (Endow et al., 1990). These results suggest a superfamily of kinesin motors in analogy to the myosins (Vale and Goldstein, 1990) against which spoke should be compared.

Irrespective of whatever sequence and/or functional homology spoke may share with other proteins, the work reported here demonstrates a major mitotic spindle structure not previously recognized. This structure is consistent with earlier models for chromosome movement in mitosis which utilize motors that span the length of the kinetochore microtubules (Pickett-Heaps et al., 1982; Nicklas, 1988; Rieder et al., 1990), including models that propose an elastic nontubulin filament network in the spindle (Pickett-Heaps et al., 1982; Leslie et al., 1987; Forer, 1988). Clearly, the kinked or possibly helical nature of the spoke-associated filament, the apparent constant number of kinks or nodes per filament, and the apparently conserved internodal distance when normalized by filament length suggest a spring-like structure. While such interpretations will certainly require direct experimental tests of spoke function, it is apparent that mechanisms for chromosome movement should now be expanded to include a role for this protein and for the novel mitotic spindle structure with which it is associated.

We are grateful to Drs. John W. Sedat and David A. Agard (Structural Biology Unit, Howard Hughes Medical Institute, San Francisco, CA) for the use of their microscope facility as well as for their advice and encouragement. We thank Karen Butner and Marc Kirschner (Department of Biochemistry and Biophysics, University of California at San Francisco) for the CREST antiserum. We also would like to thank William Earnshaw, Rick Howard, Patrick Card, Karen Butner, John Sedat, and Yasushi Hiraoka for critical reading of the manuscript. Expert technical assistance was provided by Cindy Sobotka, Rebecca Ralph, Leslie Logue, and Cheryl O'Neill.

M. R. Paddy was supported by the Howard Hughes Medical Institute.

Received for publication 31 August 1990 and in revised form 4 December 1990.

References

Agard, D. A., Y. Hiraoka, P. Shaw, and J. W. Sedat. 1989. Fluorescence microscopy in three dimensions. *Methods Cell Biol.* 30:353–377.

Belmont, A. S., J. W. Sedat, and D. A. Agard. 1987. A three-dimensional approach to mitotic chromosome structure: evidence for a complex hierarchial organization. *J. Cell Biol.* 105:77–92.

Belmont, A. S., M. B. Braunfeld, J. W. Sedat, and D. A. Agard. 1989. Large-scale structural domains within mitotic and interphase chromosomes in vivo and in vitro. *Chromosoma.* 98:129–143.

Bloom, G. S., M. C. Wagner, K. K. Pfister, and S. T. Brady. 1988. Native structure and physical properties of bovine brain kinesin and identification of the ATP-binding subunit polypeptide. *Biochemistry.* 27:3409–3416.

Burgoyne, L. A., M. A. Wagar, and M. R. Atkinson. 1971. Calcium dependent pairing of DNA synthesis in isolated rat liver nuclei. *Biochem. Biophys. Res. Commun.* 39:254–259.

Chelsky, D., R. Ralph, and G. Jonak. 1989. Sequence requirements for synthetic peptide-mediated translocation to the nucleus. *Mol. Cell. Biol.* 9: 2487–2492.

Chen, H., J. W. Sedat, and D. A. Agard. 1989. Manipulation, display, and analysis of three-dimensional biological images. *In* The Handbook of Biological Confocal Microscopy. J. Pawley, editor. IMR Press, Madison, Wisconsin. 127–135.

Cooke, C. A., M. M. S. Heck, and W. C. Earnshaw. 1987. The inner centromere protein (INCENP) antigens: movement from inner centromere to midbody during mitosis. *Cell.* 105:2053–2067.

Cooke, C. A., R. L. Bernat, and W. C. Earnshaw. 1990. CENP-B: a major human centromere protein located beneath the kinetochore. *J. Cell Biol.* 110:1475–1488.

Earnshaw, W., and N. F Rothfield. 1985. Identification of a family of centromere proteins using autoimmune sera from patients with scleraderma. *Chromosoma.* 9:313–321.

Endow, S. A., S. Henikoff, and L. Soler-Niedziela. 1990. Mediation of meiotic and early mitotic chromosome segregation in Drosophila by a protein related to kinesin. *Nature (Lond.).* 345:81–83.

Enos, A. P., and N. R. Morris. 1990. Mediation of meiotic and early mitotic chromosome segregation in Drosophila by a protein related to kinesin. *Cell.* 60:1019–1027.

Forer, A. 1988. Do anaphase chromosomes chew their way to the pole or are they pulled by actin? *J. Cell Sci.* 91:449–453.

Giloh, H., and J. W. Sedat. 1982. Fluorescence microscopy: reduced photobleaching of rhodamine and fluorescein protein conjugates by n-propyl gallate. *Science (Wash. DC).* 217:1252–1255.

Guerriero, V., Jr., D. R. Rowley, and A. R. Means. 1981. Production and characterization of an antibody to myosin light chain kinase and intracellular localization of the enzyme. *Cell.* 27:449–458.

Hay, R., M. Macy, A. Hamburger, A. Weinblatt, and T. R. Chen. 1983. Catalogue of Strains II. American Type Culture Collection, Rockville, MD. 49–50.

Hiraoka, Y., J. S. Minden, J. R. Swedlow, J. W. Sedat, and D. A. Agard. 1989. Focal points for chromosome condensation and decondensation revealed by three-dimensional in vivo time-lapse microscopy. *Nature (Lond.).* 342:293–296.

Hiraoka, Y., J. W. Sedat, and D. A. Agard. 1990. Determination of the three-dimensional imaging properties of an optical microscope system: partial confocal behavior in epi-fluorescence microscopy. *Biophys. J.* 57:325–333.

Kitagawa, T., and T. Aikawa. 1976. Enzyme-coupled immunoassay of insulin using a novel coupling reagent. *Cell.* 46:575–582.

Koshland, D. E., T. J. Mitchison, and M. W. Kirschner. 1988. Polewards chromosome movement driven by microtubule depolymerization in vitro. *Nature (Lond.).* 331:499–504.

Kuriyama, R., G. Keryer, and G. G. Borisy. 1984. The mitotic spindle of Chinese hamster ovary cells isolated in taxol-containing medium. *J. Cell Sci.* 66:265–275.

Lanford, R. E., P. Kanda, and R. C. Kennedy. 1986. Induction of nuclear transport with a synthetic peptide homologous to the SV40 T antigen transport signal. *Cell.* 46:575–582.

Leslie, R. J., R. B. Hird, L. Wilson, J. R. McIntosh, and J. M. Scholey. 1986. Kinesin is associated with a nonmicrotubule component of sea urchin mitotic spindles. *Proc. Natl. Acad. Sci. USA.* 84:2771–2775.

Meluh, P. B., and M. D. Rose. 1990. KAR3, a kinesin-related gene required for yeast nuclear fusion. *Cell.* 60:1029–1041.

Mitchison, T. J. 1988. Microtubule dynamics and kinetochore function in mitosis. *Annu. Rev. Cell Biol.* 4:527–549.

Neighbors, B. W., Jr., R. C. Williams, and J. R. McIntosh. 1988. Localization of kinesin in cultured cells. *J. Cell Biol.* 106:1193–1204.

Nicklas, R. B. 1988. The forces that move chromosomes in mitosis. *Annu. Rev. Biophys. Biophys. Chem.* 17:431–449.

Nicklas, R. B. 1989. The motor for poleward chromosome movement is in or near the kinetochore. *J. Cell Biol.* 109:2245–2254.

Paddy, M. R., A. S. Belmont, H. Saumweber, D. A. Agard, and J. W. Sedat. 1990. Nuclear envelope lamins form a discontinuous network in interphase nuclei which interacts with only a fraction of the chromatin in the nuclear periphery. *Cell.* 62:89–106.

Pepper, D. A., and B. R. Brinkley. 1977. Localization of tubulin in the mitotic apparatus of mammalian cells by immunofluorescence and immunoelectron microscopy. *Chromosoma.* 60:223–235.

Pfarr, C. M., M. Coue, P. M. Grissom, T. S. Hays, M. E. Porter, and J. R. McIntosh. 1990. Cytoplasmic dynein is localized to kinetochores during mitosis. *Nature (Lond.).* 345:263–265.

Pickett-Heaps, J. D., D. H. Tippit, and K. R. Porter. 1982. Rethinking mitosis. *Cell.* 29:729–744.

Rieder, C. L. 1982. The formation, structure, and composition of the mammalian kinetochore and kinetochore fiber. *Int. Rev. Cytol.* 79:1–19.

Rieder, C. L., S. P. Alexander, and G. Rupp. 1990. Kinetochores are transported poleward along a single astral microtubule during chromosome attachment to the spindle in newt lung cells. *J. Cell Biol.* 110:81–95.

Scholey, J. M., M. E. Porter, P. M. Grissom, and J. R. McIntosh. 1985. Identification of kinesin in sea urchin eggs, and evidence for its localization in the mitotic spindle. *Nature (Lond.).* 318:483–486.

Sedat, J., and L. Manuelidis. 1978. A direct approach to the structure of eukaryotic chromosomes. *Cold Spring Harbor Symp. Quant. Biol.* 42:331–350.

Shaw, P. J., D. A. Agard, Y. Hiraoka, and J. W. Sedat. 1989. Tilted view reconstruction in optical microscopy: three-dimensional reconstruction of Drosophila melanogaster embryo nuclei. *Biophys. J.* 55:101–110.

Steuer, E. R., L. Wordeman, T. A. Schroer, and M. P. Sheetz. 1990. Localization of cytoplasmic dynein to mitotic spindles and kinetochores. *Nature (Lond.).* 345:266–268.

Vale, R. D., and L. S. B. Goldstein. 1990. One motor, many tails: an expanding repertoire of force-generating enzymes. *Cell.* 60:883–885.

Welsh, M. J., J. R. Dedman, B. R. Brinkley, and A. R. Means. 1979. Tubulin and calmodulin. *J. Cell Biol.* 81:624–634.

Zieve, G. W., D. Turnbull, J. M. Mullins, and J. R. McIntosh. 1980. Production of large numbers of mitotic mammalian cells by use of the reversible microtubule inhibitor nocodazole. *Exp. Cell Res.* 126:397–405.